Electronic Supplementary Information

Reductively dissociable biomimetic nanoparticles for control of integrin-coupled inflammatory signaling to retard atherogenesis

Wen Gao*[a], Huazhen Yang[a], Xianghua Liu[b], Zhenhua Liu[a], Lili Tong[a], Yuhui Sun[a], Wenhua Cao[a], Yujie Cao[a] and Bo Tang*[a]

[a]College of Chemistry, Chemical Engineering and Materials Science, Collaborative Innovation Center of Functionalized Probes for Chemical Imaging in Universities of Shandong, Key Laboratory of Molecular and Nano Probes, Ministry of Education, Institute of Biomedical Sciences, Shandong Normal University, Jinan 250014, P.R. China.
[b]Ji'nan Hospital of traditional Chinese Medicine.

*Corresponding Author:
E-mail: gaowen@sdnu.edu.cn; tangb@sdnu.edu.cn.
Fax: +86 531 86180017

Contents:

Part A: Experimental Methods;

Part B: Supplementary Figures (S1-S29)

Part A: Experimental Methods

Materials. All chemicals were of analytical grade and used without further purification if not indicated otherwise. Water was purified with a Sartorius Arium 611 VF system (Sartorius AG, Germany) to a resistivity of 18.2 MΩ·cm. Bovine serum albumin (BSA) was obtained from J&K Chemicals Technology Co. Ltd. Sodium hydroxide (NaOH), Hydrochloric acid (HCl), Sodium dihydrogen phosphate (NaH_2PO_4), Dibasic Sodium Phosphate (Na_2HPO_4), Dimethylsulfoxide (DMSO), Hydrogen peroxide (H_2O_2), Methyl alcohol (CH_3OH) and Sodium dodecylsulfate (SDS) were obtained from Sinopharm Chemical Reagent. Co. Ltd. 3-(4,5-dime-thyl-thiazol-2-yl)-2,5-diphenyltetrazolium bromide (MTT) and fluorescein isothiocyanate (FITC) were purchased from Sigma-Aldrich (St. Louis, MO, USA). 4% paraformaldehyde and Triton X-100 were from Solarbio (Beijing, China). The antibodies used for western blotting included anti-integrin β_3 (PB0804), anti-YAP (PB1021) and anti-p-YAP (Ser 127, BM4580) were purchased from Boster Biological Technology Co. Ltd (Wuhan, China). β-actin (ab8227) was purchased from Abcam (Burlingame, CA, USA). Anti-JNK (AJ518) and anti-p-JNK (AJ516), polyvinylidene fluoride (PVDF) membrane, the enhanced chemiluminescence (ECL) substrate and DAPI were purchased from Beyotime Biotechnology Corporation (Haimen, China). The antibodies used for immunofluorescence included anti-CD31 and rhodamine (TRITC)-conjugated goat anti-rabbit IgG (ZF-0316) were from ZSGB-Bio (Beijing, China).

Characterization. High resolution transmission electron microscopy (HRTEM) was carried out on a JEM-2100 electron microscope. The measurements of dynamic light scattering (DLS) and zeta potential were performed on a Malvern Zeta Sizer Nano (Malvern Instruments). Absorption spectra were measured on a U-4100 UV-vis-NIR spectrophotometer (HITACHI, Japan). All pH adjustments were performed with a pH-3c digital pH-meter (Shanghai LeiCi Device Works, Shanghai, China) with a combined glass calomel electrode. Concentrations of MnO_2 were measured by inductively coupled plasma atomic emission spectroscopy (ICP-AES, Thermo). X-ray photoelectron spectra (XPS) were conducted on an ESCALAB 250xi (Thermo Fisher, USA). Scanning electron microscopy (SEM) images were taken on a Hitachi S4800 scanning electron microscope operating at 5.0 kV. Confocal fluorescence imaging studies were

performed with a TCS SP8 confocal laser scanning microscopy (Leica Co. Ltd., Germany). Absorbance in MTT assay was measured in a microplate reader (RT 6000, Rayto, USA). Imaging flow cytometry analysis was performed using an Image-Stream[X] multispectral imaging flow cytometer (Amnis Corporation) with 488 nm excitation.

Preparation and Characterization. BSA-MnO$_2$ nanoparticles were fabricated according to a biomineralization process that would induce metal ions to form metal oxide nanoclusters enveloped with protein at mild temperature.[1] In brief, 0.1 mL of MnCl$_2$ (0.1 M) was slowly added into 2 mL of BSA (5 mg/mL) solution under violent stirring. Then, NaOH (1 M) was added into the above solution to adjust pH into ≈ 11. The mixture was reacted under vigorous stirring at 37 °C for 2 h to allow the nanocrystal growth. Finally, the mixture was centrifuged by filtration (MWCO = 10 kDa, 14000 rpm, 4 °C, 30 min) to remove excess precursors, conclusively obtaining BSA-MnO$_2$ nanoparticles. EC membranes were prepared using a commercial membrane and cytosol protein extraction kit (Beyotime Biotechnology Corporation). The purified EC membranes from 1×10^8 cells were quantified by a protein assay kit (Beyotime Biotechnology Corporation). EC membrane vesicles were then formed through physically extruding on a 200 nm polycarbonate membrane for 11 passes. To coat EC membranes onto the BSA-MnO$_2$, 1 mL PBS containing BSA-MnO$_2$ was mixed with the prepared EC membrane vesicles (mass ratio of 1:1) by co-extruding on a 100 nm polycarbonate membrane for 11 passes, ultimately forming EC-BSA-MnO$_2$. BSA, EC membrane, BSA-MnO$_2$ and EC-BSA-MnO$_2$ were negatively stained with 2~3% ammonium molybdate (Sigma-Aldrich) and the morphologies of the samples were imaged by HRTEM. The protein profiles in EC-BSA-MnO$_2$ were determined by an 8% sodium dodecyl sulfate polyacrylamide gel electrophoresis (SDS-PAGE) assay and imaged by ChemiDoc™ Touch Imaging System (Bio-Rad, Hercules, CA, USA). To verify the integrity of core-shell structure of the EC-BSA-MnO$_2$ of co-localization of FITC-labeled BSA-MnO$_2$ nanoparticles and DiI (Beyotime Biotechnology Corporation)-labeled EC membranes were imaged by TCS SP8 Laser scanning confocal microscope.

Stability analysis. The EC-BSA-MnO$_2$ (100 µM) were dissolved into fetal bovine serum (FBS), cell culture medium (DMEM supplemented with 10% FBS) and PBS buffer (pH 7.4)

and kept for two weeks. Changes in size distribution and absorption peak were detected by Malvern Zeta Sizer Nano and UV-vis-NIR spectrophotometer at day 0, 2, 4, 6, 8, 10, 12, and 14. Photographs of different solutions were recorded at day 0 and 14.

Cell culture. HUVECs were purchased from Procell Life Science&Technology Co. Ltd. Rat aortic vascular smooth muscle cells (VSMCs) were obtained from Dingguo Changsheng Biotechnology Co. Ltd. The murine macrophage RAW 264.7 cells were purchased from the Committee on Type Culture Collection of the Chinese Academy of Sciences. VSMCs and RAW 264.7 cells were cultured in Dulbecco's modified Eagle medium (DMEM) containing 10% heat-inactivated FBS and 1% antibiotics penicillin/streptomycin. HUVECs were cultured in Ham's F-12K with 100 μg/mL Heparin, 50 μg/mL endothelial cell growth supplement (ECGs), 10% FBS and 1% penicillin/streptomycin. All types of cells were maintained at 37 °C in a 5% CO_2/95% air humidified incubator (MCO-15AC, SANYO).

***In vitro* homotypic target and immune escape study.** To evaluate the homotypic-targeting ability of EC-BSA-MnO_2, the HUVECs and VSMCs were incubated with FITC-labeled BSA-MnO_2 and EC-BSA-MnO_2, respectively. After 2 h incubation, adherent cells were detached from the culture plate with 0.05% Trypsin-EDTA Solution (Caisson Labs) and redispersed in PBS. A 488 nm wavelength laser was used to excite fluorescein. The fluorescence images were collected using the 500-560 nm spectral detection channels. Cell images were analyzed using IDEAS® image-analysis software (Amnis). The ability of immune-escaping was evaluated by analyzing the EC-BSA-MnO_2 uptake using the murine macrophage RAW 264.7. Cells were seeded in culture dishes with glass bottom and treated with the FITC-labeled BSA-MnO_2 or EC-BSA-MnO_2 for 2 h. Subsequently, the nuclei were stained with DAPI and observed by TCS SP8 Laser scanning confocal microscope.

Protein adsorption assay. BSA-MnO_2 and EC-BSA-MnO_2 nanoparticles were incubated with 5 mg/mL fluorescent IgG solution under continuous mixing on shaker for 2 h.[2] Next, nanoparticles were collected by centrifugation and washed with PBS for 3 times, and then redispersed in 0.5 mL PBS. The fluorescence spectra and intensity were recorded on a FLS-980 Edinburgh Fluorescence Spectrometer with a Xenon lamp with the excitation wavelength of 488 nm and the emission wavelength of 525 nm.

Cell cytotoxicity assay. HUVECs were seeded in 96-well plates at a density of 1×10^4 cells per well and cultured overnight. Then fresh medium containing different concentrations of sterilized EC-BSA-MnO$_2$ and pre-dissociated EC-BSA-MnO$_2$ (pretreatment with H$_2$O$_2$ under pH 6.5) were added. The cells grown without any treatments were used as a negative control. After incubation for 24 h, the MTT test was conducted to measure the cell viabilities relative to the untreated cells. MTT (100 μL, 0.5 mg/mL) in PBS was added and incubated at 37 °C for 4 h. The remaining MTT were eliminated by adding DMSO (100 μL) to solubilize the purple formazan crystals. Finally, the absorbance values of the cells per well were determined with a microplate reader at 490 nm for analyzing the cell viability.

***In vitro* activation of integrin-coupled inflammatory signaling.** HUVECs were seeded in 6-well cell plates or glass slides (10^6 cells/well or slide) for 24 h. Then fresh medium including sterilized (i) blank (ii) H$_2$O$_2$, (iii) EC-BSA-MnO$_2$, (iv) pre-dissociated EC-BSA-MnO$_2$ and (v) MnCl$_2$ was respectively added to each well or glass slides at concentration of 100 μM. For western blot analysis, HUVECs were homogenized in cold RIPA lysis buffer supplemented with 1 mM protease inhibitors (PMSF, Beyotime Biotechnology Corporation) after incubation for predetermined time. After scraped and centrifugation of cell lysates (4 °C,1000 rpm, 7 min), the concentration of obtaining proteins was quantified with a protein assay kit (Beyotime Biotechnology Corporation). Equal amounts of protein (50 μg) were separated by 8% SDS-PAGE gel and transferred to PVDF membrane (Bio-Rad) and blocked with blocking buffer (Beyotime Biotechnology Corporation) for 10 min. Next, membranes were incubated overnight with primary antibodies (anti-integrin β_3, 1:1,000; anti-YAP, 1:1,000; anti-p-YAP, 1:400; anti-JNK, 1:1,000; anti-p-JNK, 1:1,000) and β-actin (1:1,000), subsequently incubated 1 h with horseradish-peroxidase-conjugated secondary antibody (1:50,000). Membranes were incubated with the enhanced chemiluminescence reagent for 5 min and imaged using a ChemiDoc™ Touch Imaging system. For immunofluorescence assay, each group of cells were washed 3 time with PBS and fixed with 4% paraformaldehyde at 4 °C for 20 min. The cells were permeabilized with 0.2% Triton X-100 and blocked with normal goat serum blocking solution (ZSGB-Bio, Beijing, China) for 1 h. Then cells were incubated by primary antibody for YAP (1:400; Abcam) overnight at 4 °C. Next, tetramethylrhodamine (TRITC)-tagged

secondary antibody (1:200) was added in the dark for 1 h at room temperature. Ultimately, the nucleus was stained with DAPI for 5 min and placed into antifade mounting medium for TCS SP8 confocal laser scanning microscopy observation.

Pro-inflammatory cytokines determination. HUVECs were seeded in 12-well plates and cultured for 12 h. Then, cells were treated with 100 ng/mL PMA[3] except control group with the medium containing various substance. After incubated for 6 h, the supernatants were then collected. The levels of IL-6, IL-1β, and IL-8 in cell supernatants were analyzed using ELISA kits (Elabscience Biotech) according to the vendor's instructions.

Animals. All animal experiments were carried out according to the guidelines of the Institutional Animal Care and Use Committee (People's Republic of China). ApoE$^{-/-}$ mice (6-8 weeks old, male) were purchased from Changzhou Cavens Laboratory Animal Co. Ltd. (Changzhou, China) and housed under controlled conditions (12/12 h light/dark cycle; humidity 50-60%; 24-25 °C room temperature), with free access to water and chow. To induce the development of atherosclerotic lesions, mice were fed with the high fat diet (HFD, 20% fat, 20% sugar, and 1.25% cholesterol) for 12 weeks.

Pharmacokinetics study. Healthy ApoE$^{-/-}$ mice were randomly grouped (n = 3) and injected intravenously with FITC-labeled BSA-MnO$_2$ or EC-BSA-MnO$_2$ at 10 mg/kg. At predetermined time intervals, 20 µL of tail vein blood was collected using a tube containing heparin, and the wound was pressed for several seconds to stop the bleeding.[4] Then, fluorescence intensity of FITC in the blood was determined by an RT 6000 microplate reader. The blood circulation half-life ($t_{1/2}$) was calculated from a first order fit of the data.

Biodistribution study. To study the biodistribution of nanoparticles, plaque-bearing ApoE$^{-/-}$ mice (n = 3) were intravenously injected with FITC-labeled BSA, BSA-MnO$_2$ and EC-BSA-MnO$_2$ (10 mg/kg) via the tail vein. At 2 h post-injection, distribution of nanoparticles was detected by *ex vivo* fluorescence imaging and histology study. For *ex vivo* fluorescence imaging, aortas, heart, liver, spleen, lung and kidney from ApoE$^{-/-}$ mice were isolated and imaged by Caliper IVIS Lumina III *in vivo* small animal fluorescence imaging system (Caliper Co., USA). The fluorescence signals in each tissue were normalized to the corresponding pre-

injection baseline values. For histology study, 5-μm frozen sections of aortic roots from ApoE$^{-/-}$ mice were blocked with goat serum. Sections were incubated by primary anti-CD31 (1:400) overnight at 4°C and subsequently incubated by TRITC-tagged secondary antibody for 1 h at 37 °C. After washing 3 times with PBS, the nucleus was stained with DAPI and observed by TCS SP8 confocal laser scanning microscopy.

Anti-atherosclerotic effect study. ApoE$^{-/-}$ mice (6-8 weeks) fed high-fat diet were automatically divided into five groups (n = 6) and given an intravenous injection of (i) PBS, (ii) BSA, (iii) BSA-MnO$_2$, (iv) EC-BSA-MnO$_2$ and (v) MnCl$_2$ at 10 mg/kg dose. The injection was performed twice weekly and the body weights of mice were recorded once weekly. After 12 weeks post-injection, five groups mice were sacrificed and perfused with PBS. The peripheral fat and connective tissue were removed as much as possible. To evaluate *in vivo* inhibition of integrin-coupled inflammatory signaling, aortas from each group mice (n = 6) were homogenized on ice in lysis buffer, respectively. Changes in integrin β$_3$ expression, p-YAP/YAP and JNK/p-JNK ratio were analyzed by western blot following the same procedure as described above. The levels of IL-6, IL-1β, and IL-8 were analyzed using ELISA kits (all from Elabscience Biotech). To evaluate the accumulation of aortic macrophage, 5-μm frozen sections of aortic roots were incubated with the primary antibody for F4/80 (5 μg/mL) overnight at 4 °C. TRITC-labeled secondary antibody (1:200) was added and the sections were incubated in the dark for 1 h. Finally, the nucleus was stained with DAPI and observed by confocal microscopy.

To analyze the extent of atherosclerotic lesion, two methods were used. For *en face* analysis, whole aortas were opened longitudinally and stained with Oil red O. Photographs of the stained specimens were digitized for data analysis. The luminal lesion surface area was quantified by using NIS-Elements imaging software (Nikon, Japan). Data were expressed as the percentage of the aorta with positive Oil red O staining. For histological analysis, the upper sections of hearts from each group mice were embedded in paraffin, and 5 μm-thick serial sections were prepared. Every section was stained with Oil red O and haematoxylin. Photographs were digitized by using Leica Stereozoom microscope M205 A (Leica Microsystems, Singapore). For *in vivo* toxicity study, major organs of mice from five group

were collected and sliced for haematoxylin and eosin (H&E) staining. Images were captured using a Leica DMI3000 microscope with a ×20 objective lens (Leica Microsystems, Wetzlar, GmbH).

Statistical Analysis. Each experiment was repeated three times in duplicate if not stated otherwise. Data were presented as mean ± S.D. Comparisons between groups were analyzed using Student's t-test, $P < 0.05$ was considered statistically significant.

References

1.   L. Tian, Q. Chen, X. Yi, J. Chen, C. Liang, Y. Chao, K. Yang and Z. Liu, *Small*, 2017, **13**.

2.   G. Cheng, W. Li, L. Ha, X. Han, S. Hao, Y. Wan, Z. Wang, F. Dong, X. Zou, Y. Mao and S. Y. Zheng, *J. Am. Chem. Soc.*, 2018, **140**, 7282-7291.

3.   Y. Dou, Y. Chen, X. Zhang, X. Xu, Y. Chen, J. Guo, D. Zhang, R. Wang, X. Li and J. Zhang, *Biomaterials*, 2017, **143**, 93-108.

4.   W. Gao, Y. Zhao, X. Li, Y. Sun, M. Cai, W. Cao, Z. Liu, L. Tong, G. Cui and B. Tang, *Chem. Sci.*, 2018, **9**, 439-445.

Part B: Supplementary Figures
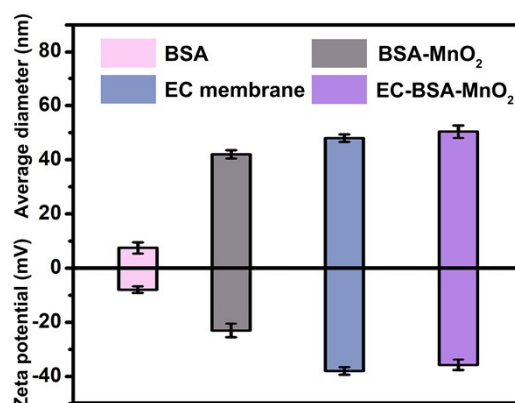
Figure S1. Changes in the particle size and zeta potential of BSA, BSA-MnO$_2$, EC membrane and EC-BSA-MnO$_2$. Data are shown as the mean ± S.D. (n = 3).
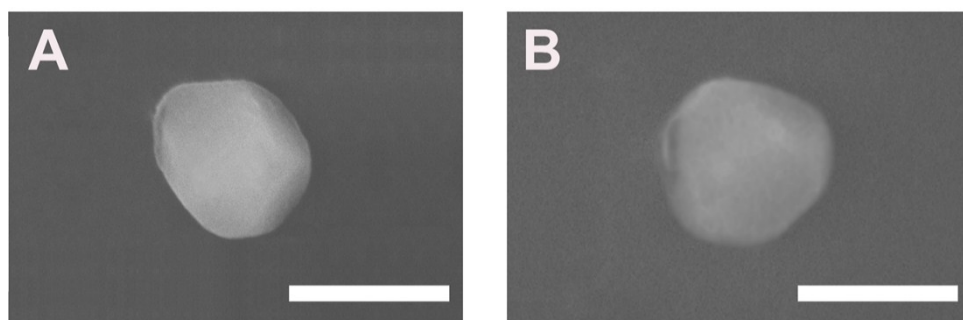
Figure S2. SEM images of (A) BSA-MnO$_2$ and (B) the EC-BSA-MnO$_2$. Scale bar = 50 nm.
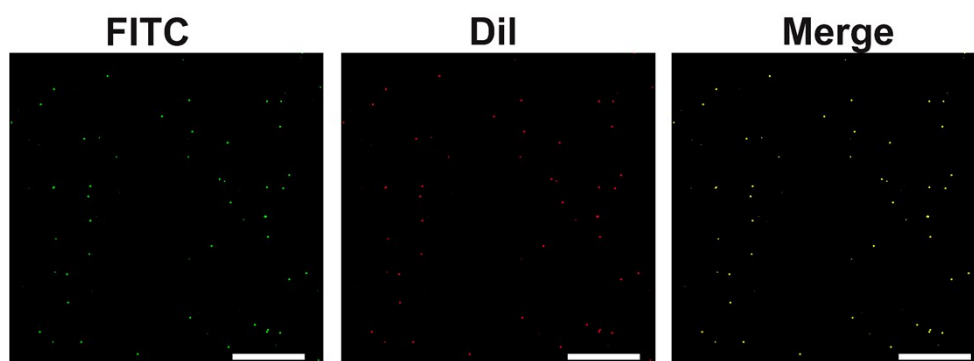
Figure S3. Confocal images of EC-BSA-MnO$_2$. EC membranes were labeled with DiI (red) and BSA-MnO$_2$ were labeled with FITC (green) for imaging. Scale bar = 10 μm.
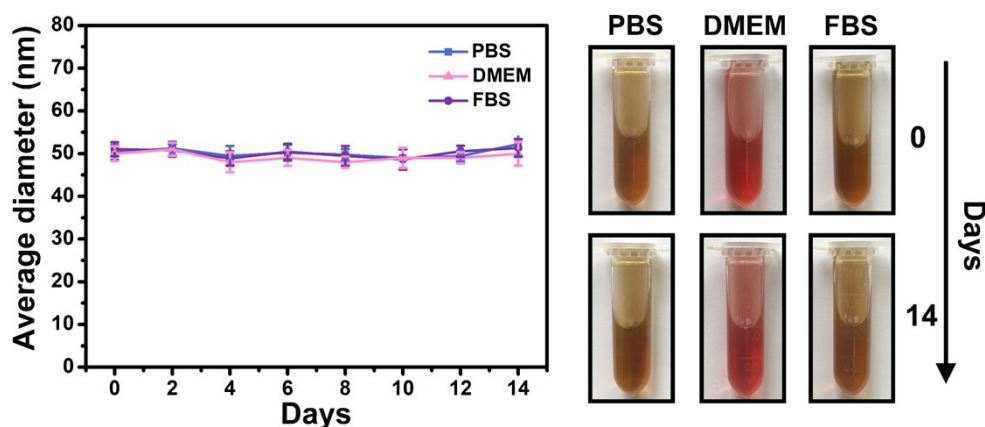
Figure S4. The stability of EC-BSA-MnO$_2$. DLS data (left) of nanoparticles dispersed in PBS, FBS and cell culture medium (DMEM supplemented with 10% FBS) for 14 days and photographs (right) of the nanoparticle dispersed in PBS, FBS and cell culture medium (DMEM supplemented with 10% FBS) for 14 days. Data are shown as mean ± S.D. (n = 3).
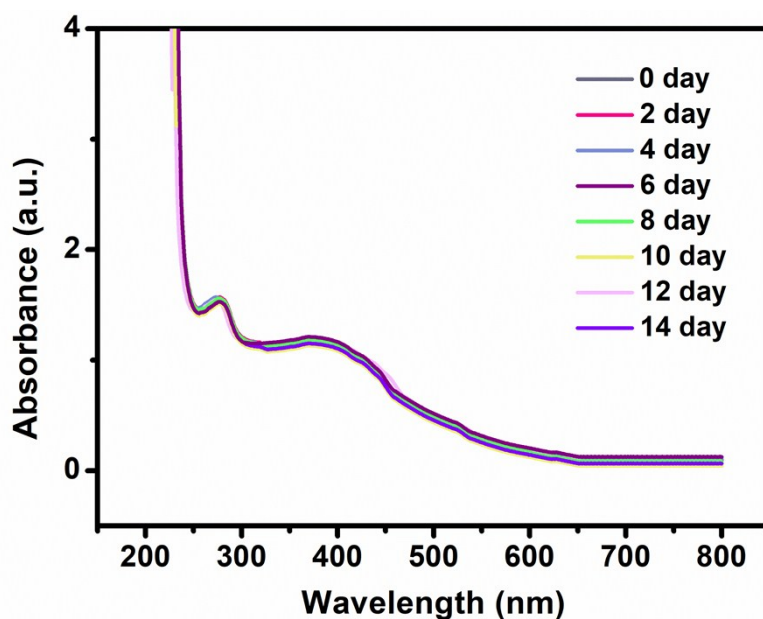
Figure S5. UV-Vis-NIR absorbance spectra of EC-BSA-MnO$_2$ dispersed in PBS buffer (pH 7.4) for 14 days.
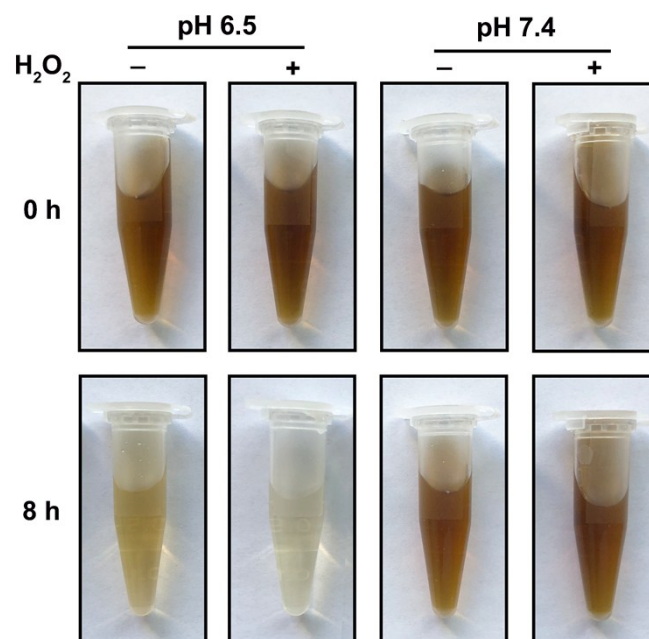
Figure S6. Photographs of EC-BSA-MnO$_2$ dispersed in pH 6.5 or pH 7.4 solutions with or without H$_2$O$_2$ at 0 h and 8 h.
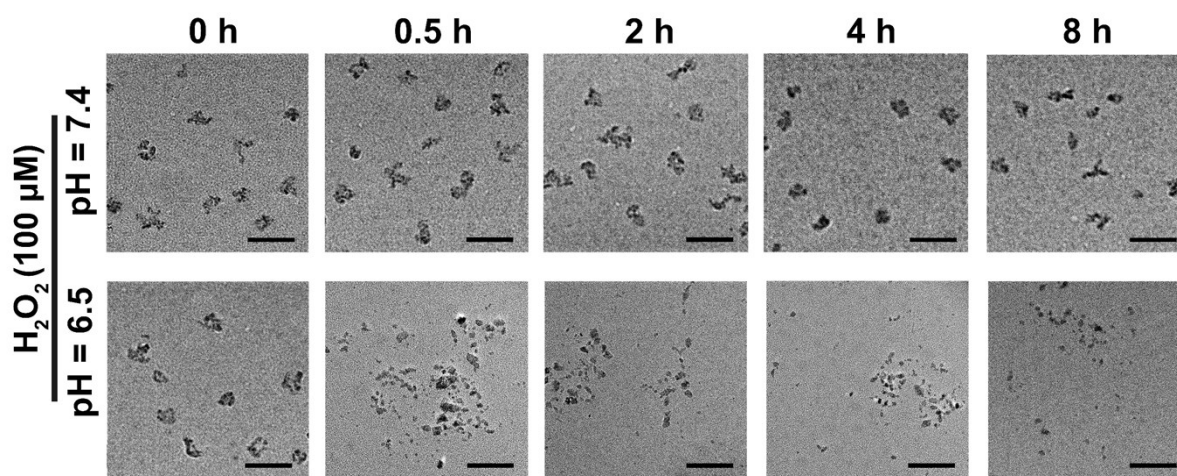
Figure S7. TEM images of EC-BSA-MnO$_2$ in PBS (pH 6.5 and 7.4) with 100 μM H$_2$O$_2$. Scale bar = 100 nm.
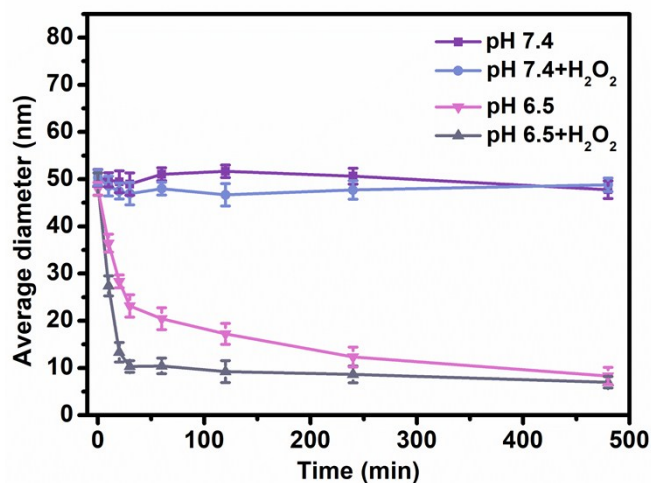
Figure S8. The degradation behavior of EC-BSA-MnO$_2$ dispersed in buffers with different pH values (7.4 and 6.5) with or without H$_2$O$_2$ measured by DLS. Data are shown as mean ± S.D. (n = 3).
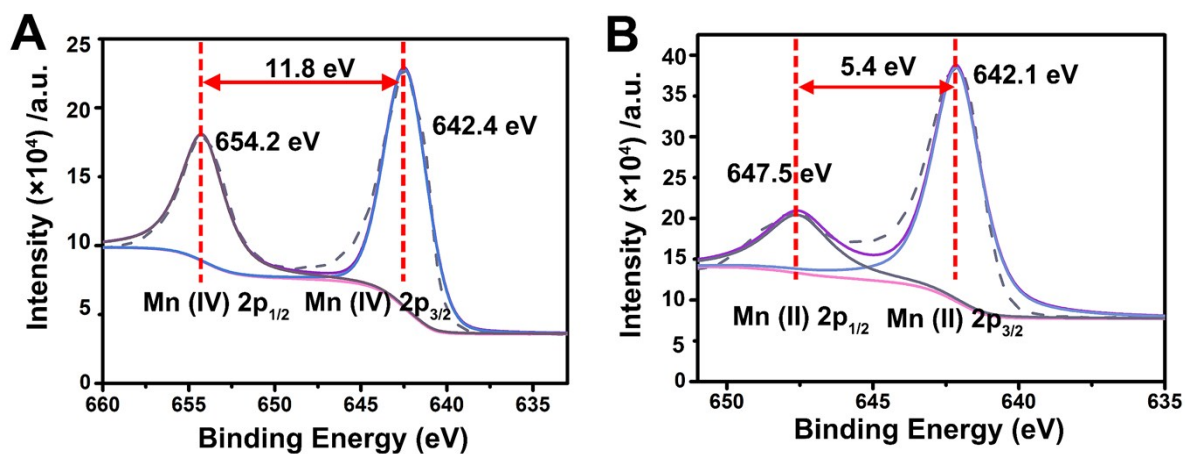
Figure S9. Mn 2p XPS spectrum of EC-BSA-MnO$_2$ before (A) and after (B) decomposition.
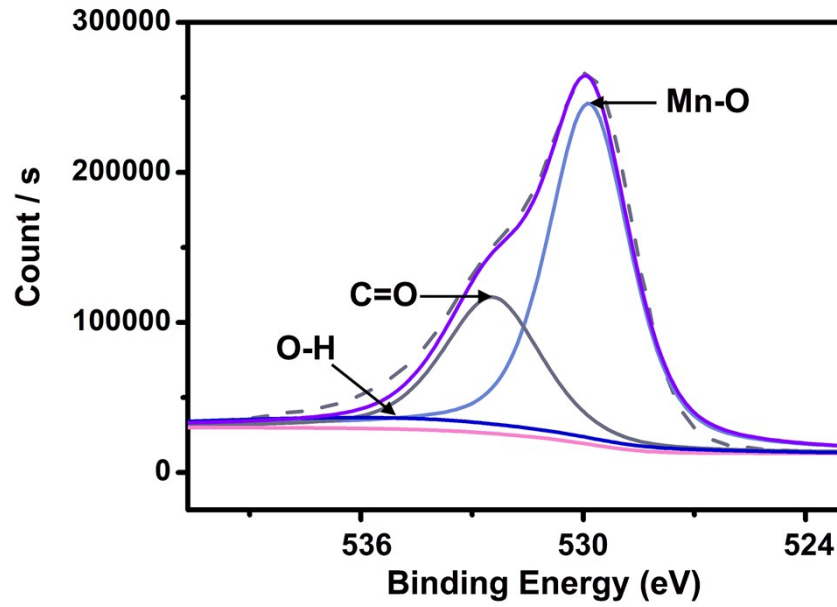
Figure S10. O 1s XPS spectra of EC-BSA-MnO$_2$.
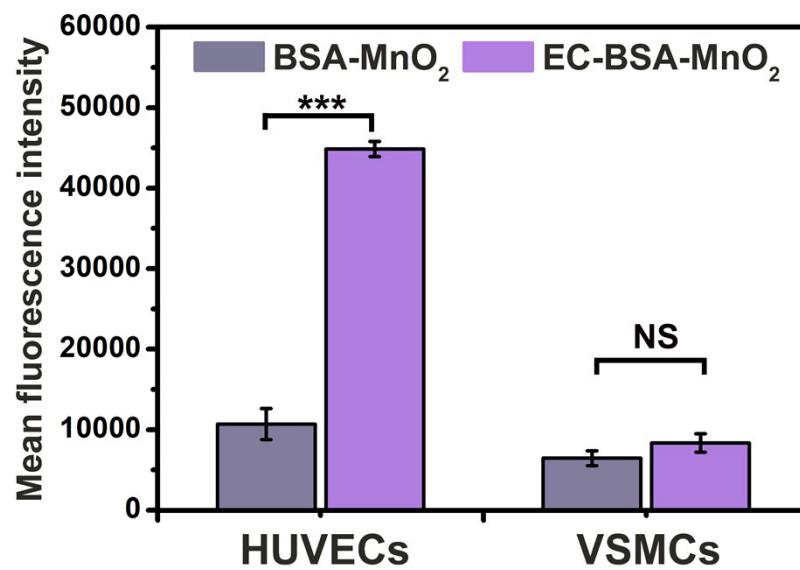
Figure S11. Mean membrane intensity of BSA-MnO$_2$ (red area: 10687.56) was 23.8% of EC-BSA-MnO$_2$ (red area: 44879.72) in HUVECs. No significant difference was found in VSMCs. Data are shown as mean ± S.D. (n = 3), and analyzed by Student's *t*-test. [***]$P < 0.001$.
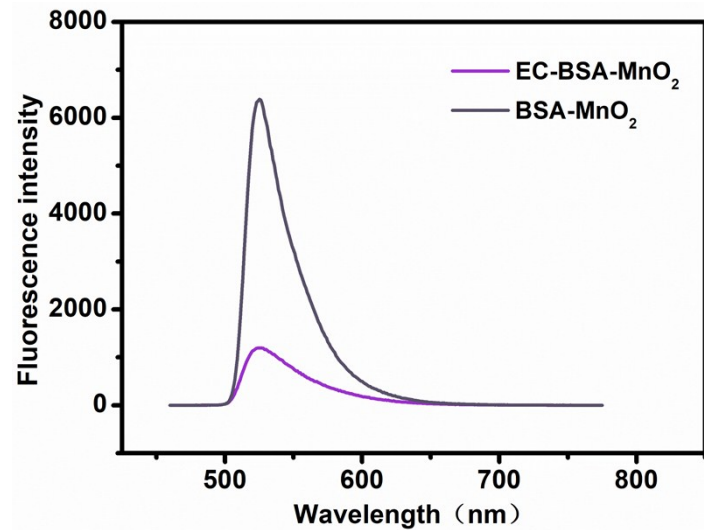
Figure S12. Fluorescence spectra of fluorescent IgG absorbed on BSA-MnO$_2$ and EC-BSA-MnO$_2$ nanoparticles.
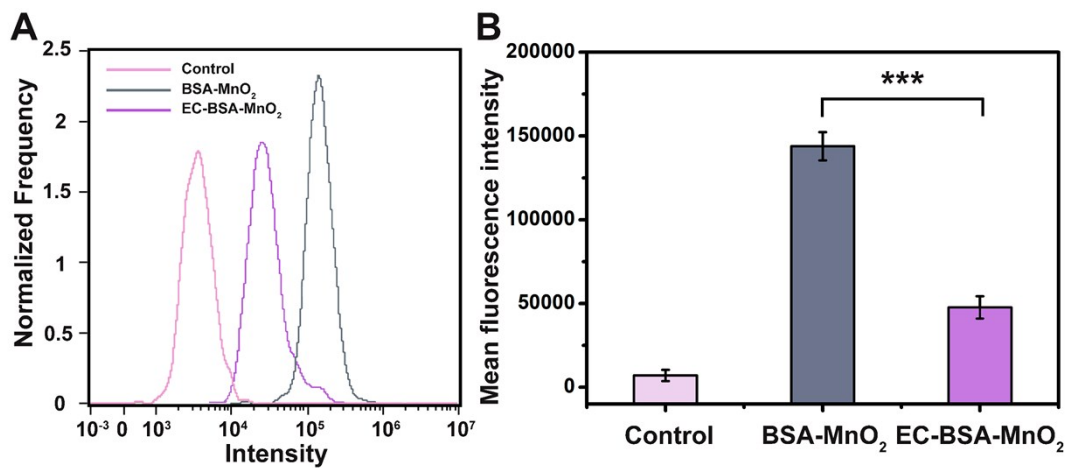
Figure S13. (A) Flow cytometry analysis of RAW 264.7 cells incubated with BSA-MnO$_2$ and EC-BSA-MnO$_2$ nanoparticles for 2 h. (B) Quantification of the mean fluorescence intensity of the RAW 264.7 cell uptake. Data are shown as mean ± S.D. (n = 3), and analyzed by Student's *t*-test. ***$P < 0.001$.
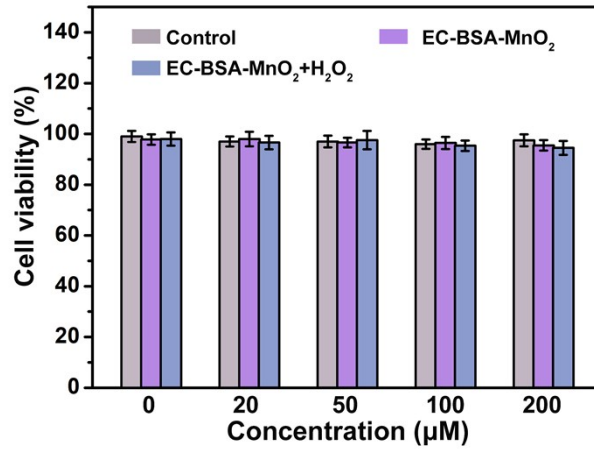
Figure S14. The viability of HUVECs after treatment with various concentrations of EC-BSA-MnO$_2$ and pre-disaggregated EC-BSA-MnO$_2$ for 24 h.
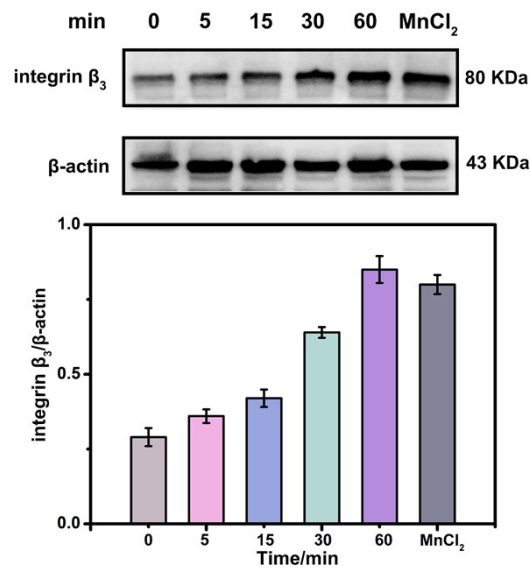
Figure S15. Western blot analysis of the integrin β$_3$ expression in HUVECs treatment with pre-dissociated EC-BSA-MnO$_2$ (100 μM, pretreatment with 100 μM H$_2$O$_2$ under pH 6.5) at predetermined time intervals. The relative levels of integrin β$_3$ was normalized using β-actin. Data are shown as mean ± S.D. (n = 3).
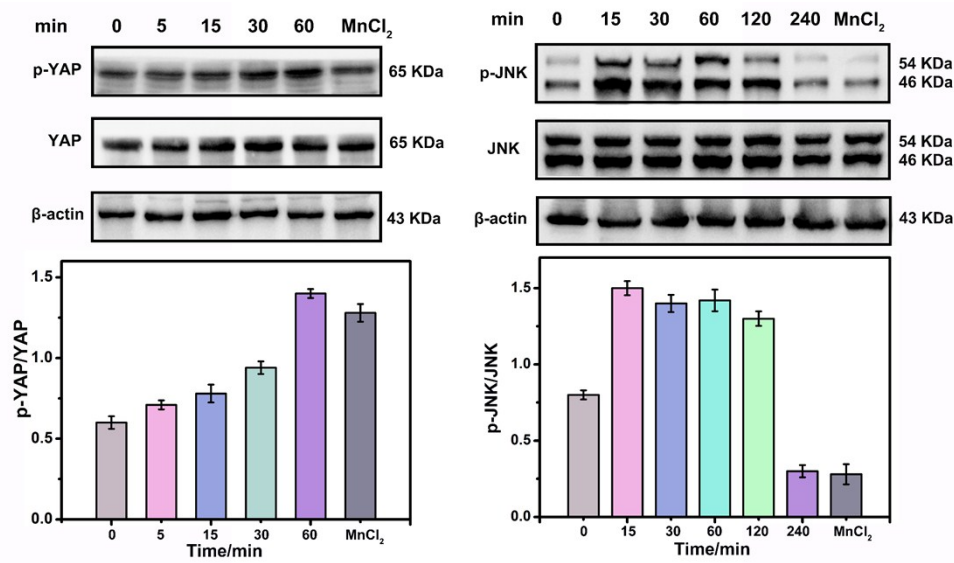
Figure S16. Western blot analysis of the expression of YAP and JNK phosphorylation in HUVECs with treatment of pre-dissociated EC-BSA-MnO$_2$ (100 µM, pretreatment with 100 µM H$_2$O$_2$ under pH 6.5) at predetermined time intervals. The relative levels of YAP and JNK phosphorylation were normalized to total YAP and JNK, with β-actin serving as a loading control. Data are shown as mean ± S.D. (n = 3).
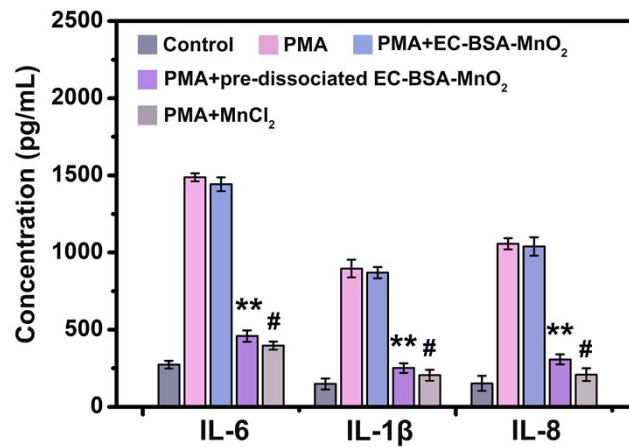

Figure S17. Cytokine levels in PMA-stimulated HUVECs after different treatments. Data are shown as mean ± S.D. (n = 3), and analyzed by Student's *t*-test. [**]*P* < 0.01 for pre-dissociated EC-BSA-MnO$_2$ *vs*. PMA group. [#]*P* < 0.05 for MnCl$_2$ *vs*. PMA group.
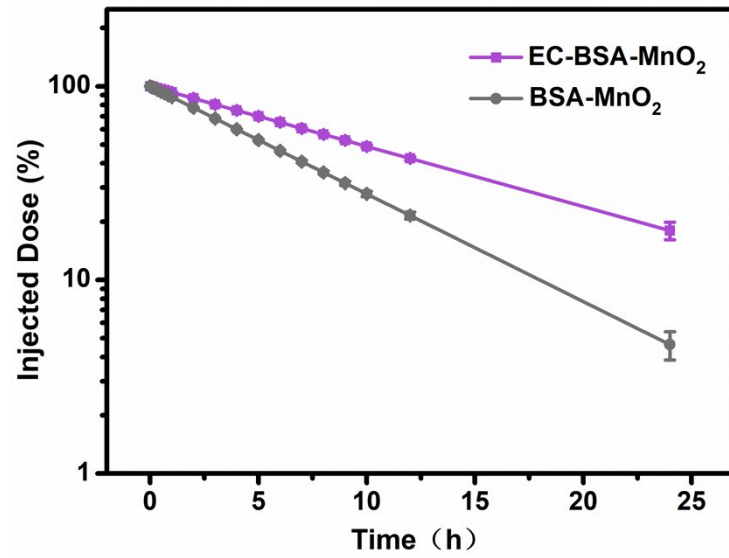
Figure S18. Pharmacokinetics of EC-BSA-MnO$_2$ and BSA-MnO$_2$. Data are shown as mean $\pm$ S.D. (n = 3).
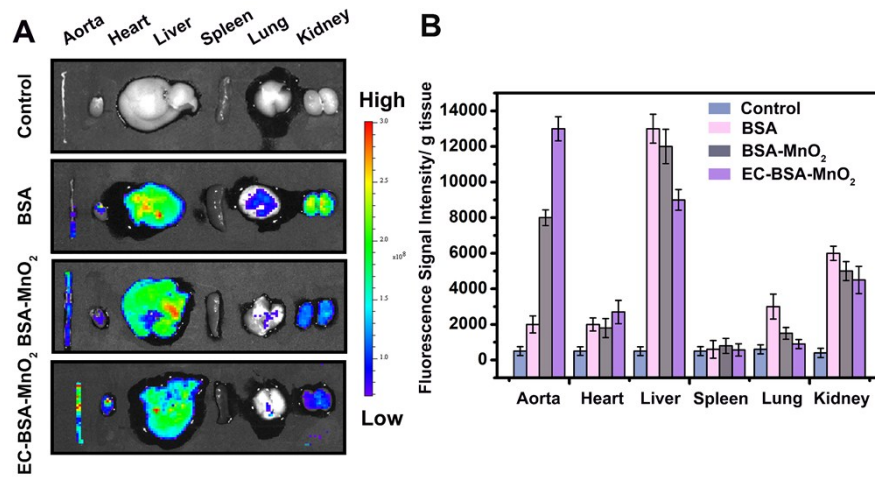

Figure S19. (A) Representative fluorescence images of the aortas and main organs of the plaque-bearing ApoE$^{-/-}$ mice sacrificed after 2 h injection of control, BSA, BSA-MnO$_2$ and EC-BSA-MnO$_2$. (B) Quantification of the fluorescence intensity in the tissues. Data are shown as the mean $\pm$ S.D. (n = 3).

Healthy aortas

EC-BSA-MnO$_2$

BF | CD31 | FITC | DAPI | Merge
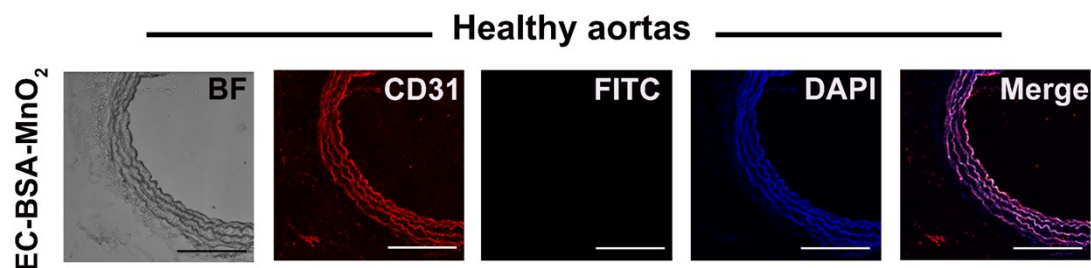
Figure S20. Representative immunofluorescent micrographs of EC-BSA-MnO$_2$ accumulation in healthy aortas. From right, merge, blue (DAPI), green (FITC-labeled EC-BSA-MnO$_2$) and red (HUVECs maker CD31). Scale bar = 75 μm.
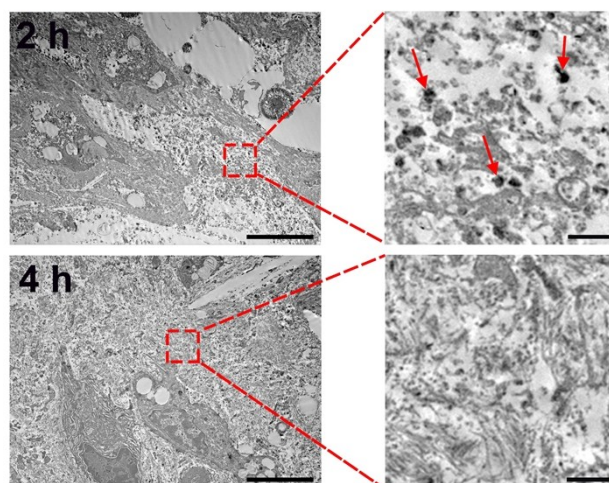

Figure S21. Representative TEM images of plaque cross-sections of the ApoE$^{-/-}$ mice. Scale bar = 5 μm. Red arrows indicated the localization of EC-BSA-MnO$_2$ in plaque section. The red dashed square represents the amplifying image of a region of lesion as indicated on the right. Scale bar = 200 nm. (n = 3).
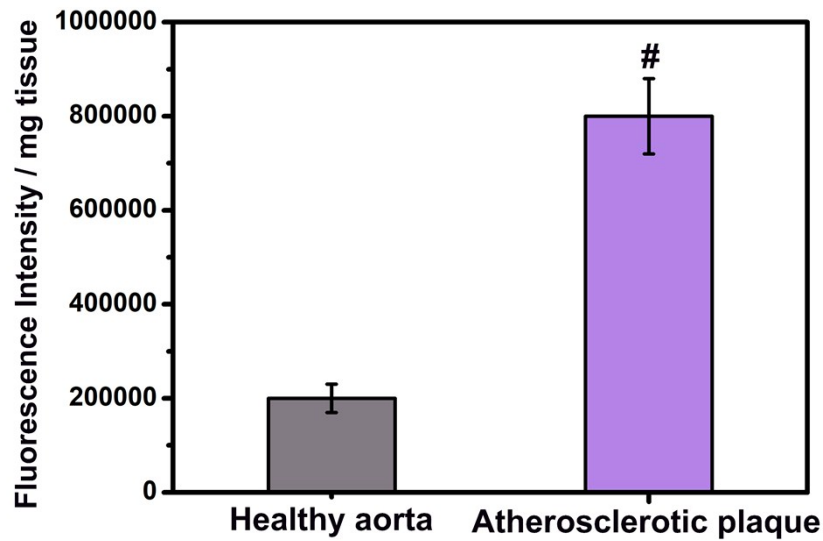
Figure S22. Levels of H_2O_2 in atherosclerotic plaque. Tissue extracts were isolated from healthy aortas or atherosclerotic plaques, measured by Mito-NIRHP (10 µM, 10 min) and expressed as fluorescence intensity per mg of tissue weight. Data are shown as mean ± S.D. (n = 3), and analyzed by Student's *t*-test. [#]$P < 0.05$.
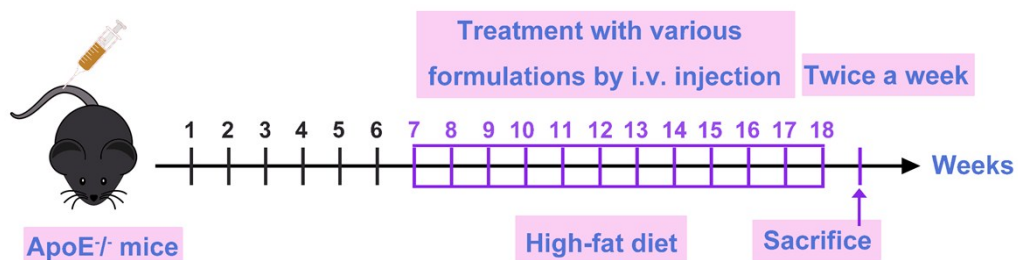

**Figure S23.** Schematic illustration of the treatment protocols.
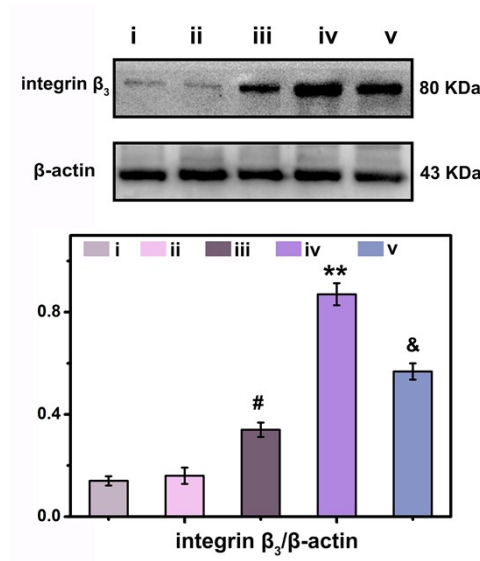
Figure S24. Western blot analysis of integrin β_3 in the aortic arch lesions from high-fat diet-fed ApoE$^{-/-}$ mice. Mice were treated with (i) PBS, (ii) BSA, (iii) BSA-MnO$_2$, (iv) EC-BSA-MnO$_2$, (v) MnCl$_2$ for 12 weeks. Each of treatments were used at the same dose of 10mg/kg. The relative levels of integrin β_3 was normalized using β-actin. Data are shown as mean ± S.D. (n = 6), and analyzed by Student's t-test. **$P < 0.01$ for EC-BSA-MnO$_2$ vs. PBS, #$P < 0.05$ for MnCl$_2$ vs. PBS, &$P < 0.05$ for EC-BSA-MnO$_2$ vs. MnCl$_2$.
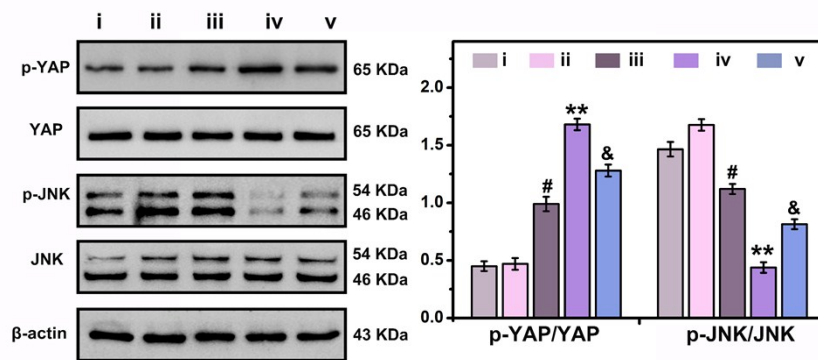

Figure S25. Western blot analysis of phosphorylation of YAP and JNK in the aortic arch lesions from high-fat diet-fed ApoE$^{-/-}$ mice. Treatments as indicated in Figure S24. The relative levels of YAP and JNK phosphorylation were respectively normalized to total YAP and JNK, with β-actin serving as a loading control. Data are shown as mean ± S.D. (n = 6), and analyzed by Student's t-test. **$P < 0.01$ for EC-BSA-MnO$_2$ vs. PBS, #$P < 0.05$ for MnCl$_2$ vs. PBS, &$P <$ 0.05 for EC-BSA-MnO$_2$ vs. MnCl$_2$.
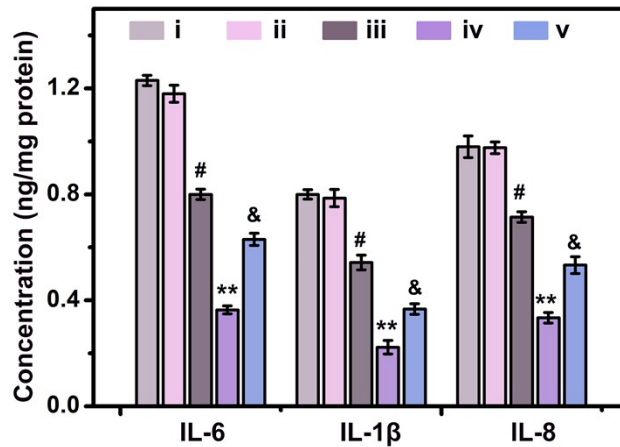
Figure S26. Levels of IL-6, IL-1β and IL-8 in aortic tissues from ApoE$^{-/-}$ mice treated with different formulations. Treatments as indicated in Figure S24. Data are shown as mean ± S.D. (n = 6), and analyzed by Student's *t*-test. $^{**}P < 0.01$ for EC-BSA-MnO$_2$ *vs*. PBS, $^{\#}P < 0.05$ for MnCl$_2$ *vs*. PBS, $^{\&}P < 0.05$ for EC-BSA-MnO$_2$ *vs*. MnCl$_2$.
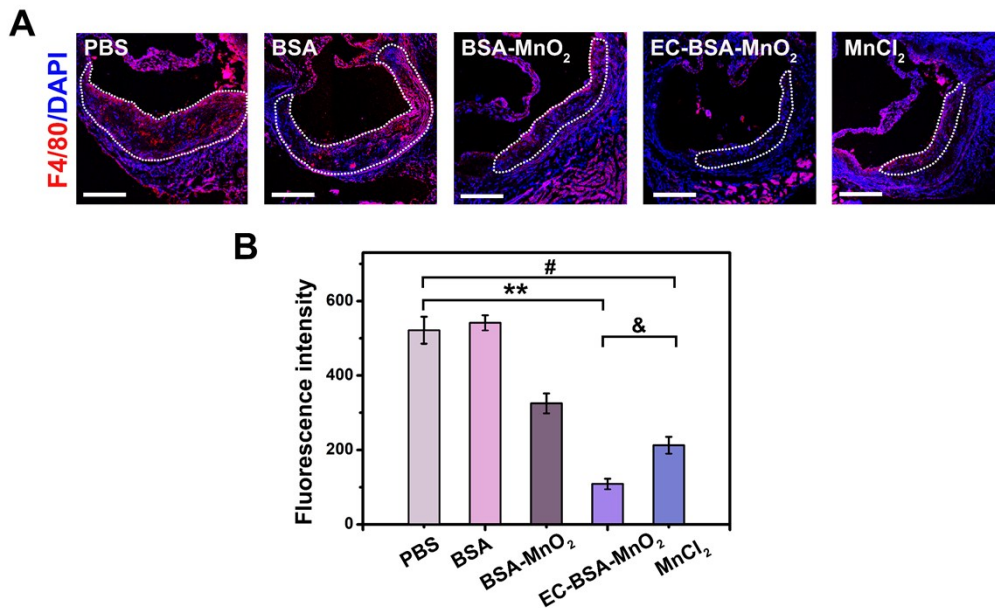
Figure S27. (A) Representative immunofluorescence micrographs of aortic roots sections of PBS, BSA, BSA-MnO$_2$, EC-BSA-MnO$_2$ and MnCl$_2$-treated animals. Macrophages were stained with F4/80 (red) and cell nuclei were stained with DAPI (blue). Scale bar = 100 μm. The white dashed line indicates the plaque border. (B) Quantification of fluorescence intensity from F4/80 in the lesion area of aortic root. Data are shown as mean ± S.D. (n = 6), and analyzed by Student's *t*-test. $^{**}P < 0.01$ for EC-BSA-MnO$_2$ *vs*. PBS, $^{\#}P < 0.05$ for MnCl$_2$ *vs*. PBS, $^{\&}P < 0.05$ for EC-BSA-MnO$_2$ *vs*. MnCl$_2$.
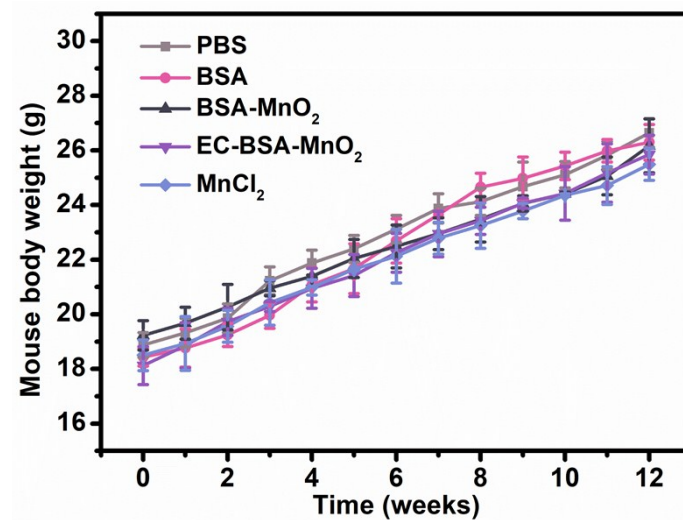
Figure S28. 12-week growth chart of high-fat diet-fed ApoE$^{-/-}$ mice received as indicated treatment. Data are shown as mean ± S.D. (n = 6). No statistical significance was detected.
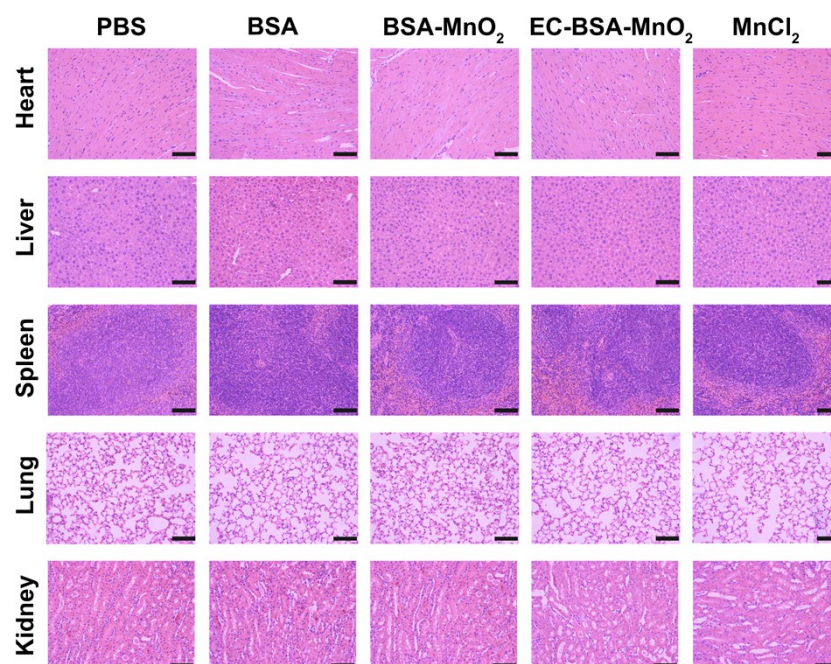
Figure S29. Representative histology (H&E) images of major organs collected from high-fat diet-fed ApoE$^{-/-}$ mice receiving treatments as indicated after 12 weeks. No noticeable abnormality was found in the heart, liver, spleen, lung, or kidney. Scale bar = 100 μm.